

Seismology based Strong Ground Motion Attenuation Relationship for Tohoku Area in Japan



Z.R. Tao, X.X. Tao & A.P. Cui

Key Laboratory of Earthquake Engineering and Engineering Vibration, Institute of Engineering Mechanics, CEA

X.X. Tao

Harbin Institute of Technology, China

ABSTRACT:

A seismology based approach, to establish strong ground motion attenuation relationships for regions with few or without strong ground motion records, is developed. Tohoku area in Japan, with rich records, is selected as the target area to verify the feasibility. Data from small earthquakes, recorded by F-net seismographs, are adopted to calculate the Fourier spectra. The envelopes of these spectra are taken as the objectives to inverse five regional source and crustal medium parameters by micro-genetic algorithm, including stress drop, the parameters of intrinsic attenuation and the parameters of the geometrical spreading function. These parameters are adopted to calculate a Fourier amplitude spectrum, and a complex spectrum is formed by combining a random phase spectrum and the amplitude spectrum. An acceleration time history can be simulated, and PGAs on different distances are obtained. The primary results are compared with K-NET records and some empirical attenuation relationships.

Keywords: attenuation relationship, inversion, regional parameters

1. INTRODUCTION

For most countries and regions, strong ground motion records are not enough to establish strong ground motion attenuation relationships by empirical methods. An approach, which is based on seismology, is developed to estimate strong ground motion for these regions. To test the feasibility, Tohoku area in Japan is selected as the target area, since the activity is high and there are some references on source and regional parameters.

It is well known that small earthquakes are much more and easier to be recorded. Records from the digital broadband seismograph network F-net in small earthquakes are adopted to inverse the source and regional parameters by the micro-Genetic Algorithm. These parameters describe the characteristics of the source area and path medium, and the relation with the size of earthquakes is not close. After taking these parameters into Brune ω^2 source spectrum, a complex spectrum can be formed by combining a random phase spectrum and this amplitude spectrum. An acceleration time history is then obtained and windowed, and it is transformed to the frequency domain and normalized. This complex spectrum is transformed back to the time domain. On each distance, the median PGA of 50-times calculation is adopted to form the attenuation relationship. This relationship for each magnitude is compared with strong ground motion records from K-NET and some empirical relationships.

2. DATABASE

Tohoku area (N36°-40°, E138°-143°) is selected as the target area, in which there are 12 F-net stations, as shown in Fig. 2.1.

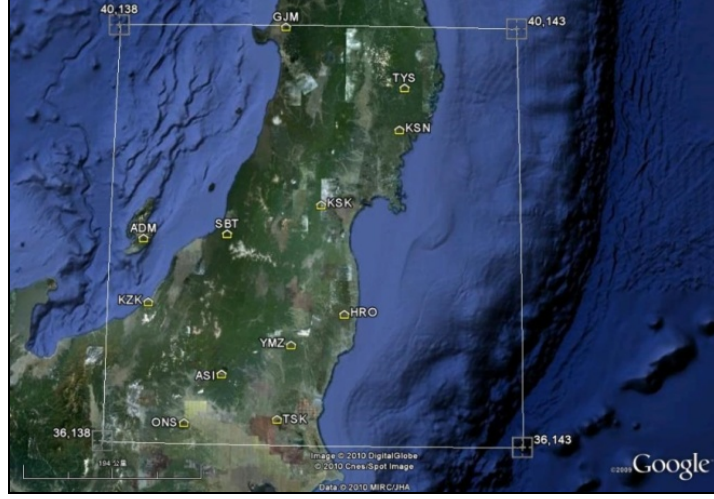


Figure 2.1. F-net stations distribution

Envelops of 850 records from 632 small earthquakes ($M_w=3.5-4.5$, focal depth ≤ 30 km, Jan. 1996-Oct. 2010) are adopted as the objective function for inversion. The distribution of these records with hypocentral distance and focal depth is shown in Fig. 2.2.

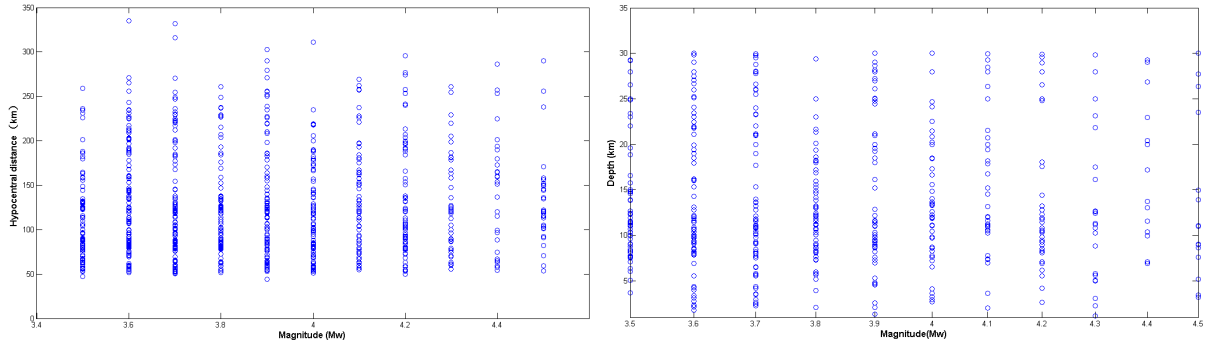


Figure 2.2. F-net records distribution

For comparison, there are 4189 records from destructive earthquakes ($4.5 \leq M_w \leq 7.5$, focal depth ≤ 30 km), recorded by rock-site K-NET stations in this area. The magnitude used in K-NET records is M_{JMA} , which is converted to M_w by Eqn. 2.1 (Takamura, 1990) and Eqn. 2.2 (Hanks and Kanamori, 1979).

$$\log M_0 = 1.17 M_{JMA} + 17.72 \quad (2.1)$$

$$\log M_0 = 1.5 M_w + 16.1 \quad (2.2)$$

3. SIMULATION OF ACCELERATION TIME HISTORY

Assuming that the far-field accelerations on an elastic half space are band-limited, finite-duration and white Gaussian noise, and the approach is based on Brune ω^2 source spectrum, the Fourier spectrum on a site can be presented as (Boore, 2003),

$$FA(M_0, f, R) = \frac{R_{\theta\theta} FV}{4\pi R_0 \rho_s \beta_s^3} \times \frac{M_0}{1 + \left(\frac{f}{f_0}\right)^2} \times e^{-\frac{\pi f R}{Q(f)\beta_s}} \times \frac{1}{\left[1 + \left(\frac{f}{f_{\max}}\right)^8\right]^{-1/2}} \times (2\pi f)^z \times G(R) \times A(f) \quad (3.1)$$

where, $R_{\theta\phi}$ is the radiation pattern of the shear excitation, with the assumption that the energy was equally partitioned into two horizontal components; F is the free surface effect; V is the vectorial partitioning of shear wave energy into two components of equal amplitude; R_0 is a reference distance; ρ_s is the density in the vicinity of the source; β_s is the shear-wave velocity in the vicinity of the source; M_0 is the seismic moment; f is the frequency; f_0 is the corner frequency, $f_0 = 4.9 \times 10^6 \times \beta_s \times (\Delta\sigma / M_0)^{1/3}$, $\Delta\sigma$ is the stress drop; f_{max} is the high-frequency cutoff frequency; z is the index variable, $z=0, 1$ and 2 is for displacement, velocity and acceleration; R is the hypocentral distance; $Q(f)$ is the function of frequency, which describes the crustal medium, $Q(f)=Q_0 f^\eta$; $G(R)$ is the geometric spreading function; $A(f)$ is the amplification factor of near surface amplitude as a function of hypocentral distance R and frequency f .

In this equation, $\Delta\sigma$, Q_0 , η and two parameters R_1 and R_2 of $G(R)$ are inverted by Micro-Genetic Algorithm (μ GA), since they are considered as unrelated with the size of earthquakes. These are to describe the source and the medium during wave propagation. The objective function is the residual sum of squares between the calculated Fourier spectrum (Eqn. 3.1) and the objective spectrum from observed records, which is

$$\phi_j = \sum_m \sum_n [FA_0(m, n) - FA_j(m, n)]^2 \quad (3.2)$$

where, m is observed records; n is the points on a Fourier spectrum; FA_0 is the objective Fourier spectrum; FA_j is the calculated Fourier spectrum from generation j .

Fitness is calculated from the objective function by Eqn. 3.3, which is between 0 and 1.

$$F_j = e^{-\beta\phi_j} \quad (3.3)$$

where, β is the fitness coefficient, which effects the evolution of the μ GA to a large extent.

In this inversion, the ranges of inverse parameters (Tao et al., 2012) and the optimum solution, after searching among 2000 generations, are listed in Table 3.1.

Table 3.1. Inverse results

$\Delta\sigma$ [bars]	Q_0	η	R_1 [km]	R_2 [km]
70-150	150-300	0.6-1.0	50-100	100-150
75	153	0.96	95	121

These results are taken to obtain ground motions. Combined with a random phase spectrum, the Fourier spectrum (Eqn. 3.1) can be transformed into the time domain, and PGAs on each distance can be picked. Fifty acceleration time histories are simulated and the average values are adopted. In time-domain simulations (Boore, 2003), these time series are windowed by

$$f(t) = \begin{cases} (t/t_1)^2, & 0 \leq t \leq t_1 \\ 1.0, & t_1 < t \leq t_2 \\ e^{-c(t-t_2)}, & t_2 < t \end{cases} \quad (3.4)$$

where, t_1 and t_2 are the starting point and finishing point of the stable section, c is the attenuation rate. And in this paper, Eqn. 3.5 (Huo and Hu, 1991) is adopted, which is the envelop curve on bedrock.

$$\begin{cases} \lg t_1 = -1.074 + 1.005 \lg(R + 10) \\ \lg t_2 = -2.268 + 0.3262M_w + 0.5815 \lg(R + 10) \\ \lg c = 1.941 - 0.2817M_w - 0.5870 \lg(R + 10) \end{cases} \quad (3.5)$$

The windowed time histories are transformed into the frequency domain, and the real and the imaginary parts are normalized by the modulus. Then, the complex spectra are transformed back to the time domain. Attenuation curves, which show mean levels, can be constructed after mean PGAs from 50 different random phase spectra are calculated.

4. COMPARISONS

Strong ground motion attenuation relationships obtained above are compared with strong ground motion records and some empirical relationships, as shown in Fig. 4.1. Strong ground motion records are from K-NET stations on bedrock and some empirical relations (Fukushima and Tanaka, 1990; Kanno et al., 2006; Si and Midorikawa, 2000).

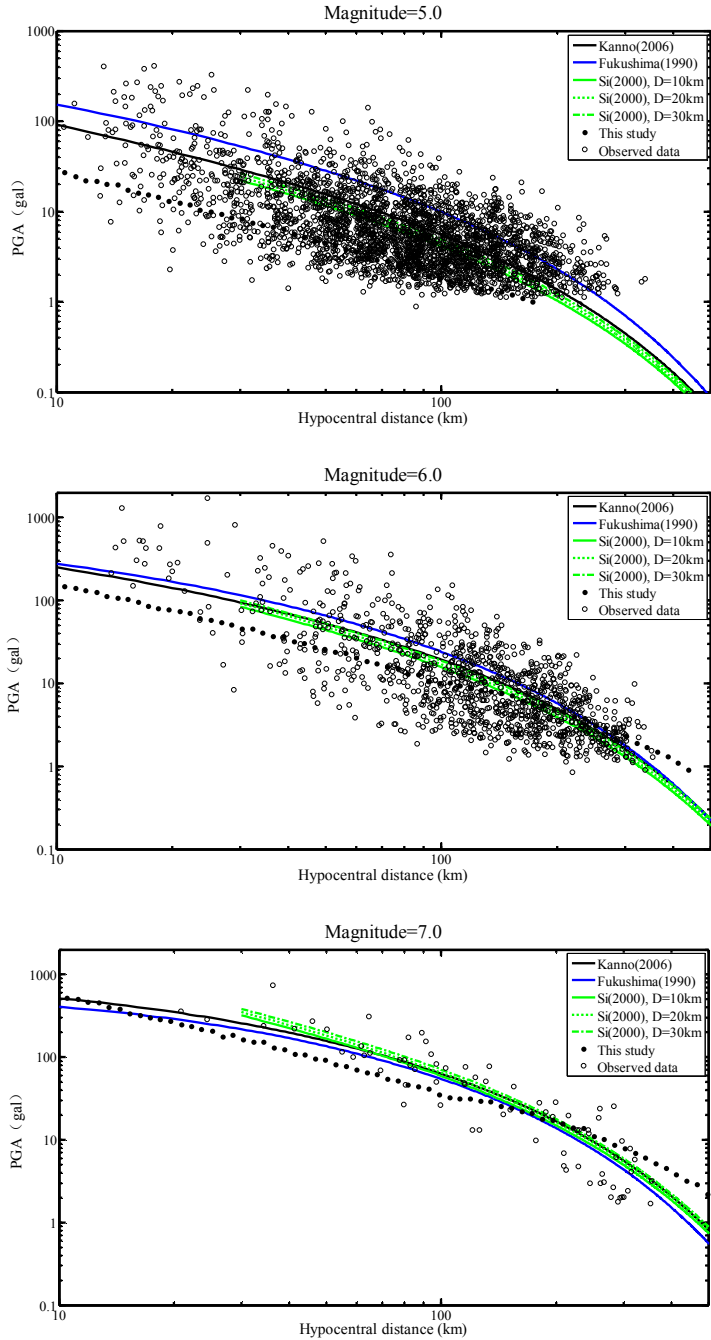


Figure 4.1. Comparison on attenuation relationships

It is shown that the results are closer to empirical relations on far fields (hypocentral distance > 100 km), and on the medium field, they are lower than those relations. Comparisons between the mean residuals and standard deviations, defined by Eqn. 4.1, from this study and empirical relations are shown in Table 4.1. Distributions of the mean residuals with hypocentral distance are shown in Figure 4.2. These data are separated into three groups, $4.5 \leq M_w < 5.5$ ($M_w=5$), $5.5 \leq M_w < 6.5$ ($M_w=6$) and $6.5 \leq M_w \leq 7.5$ ($M_w=7$).

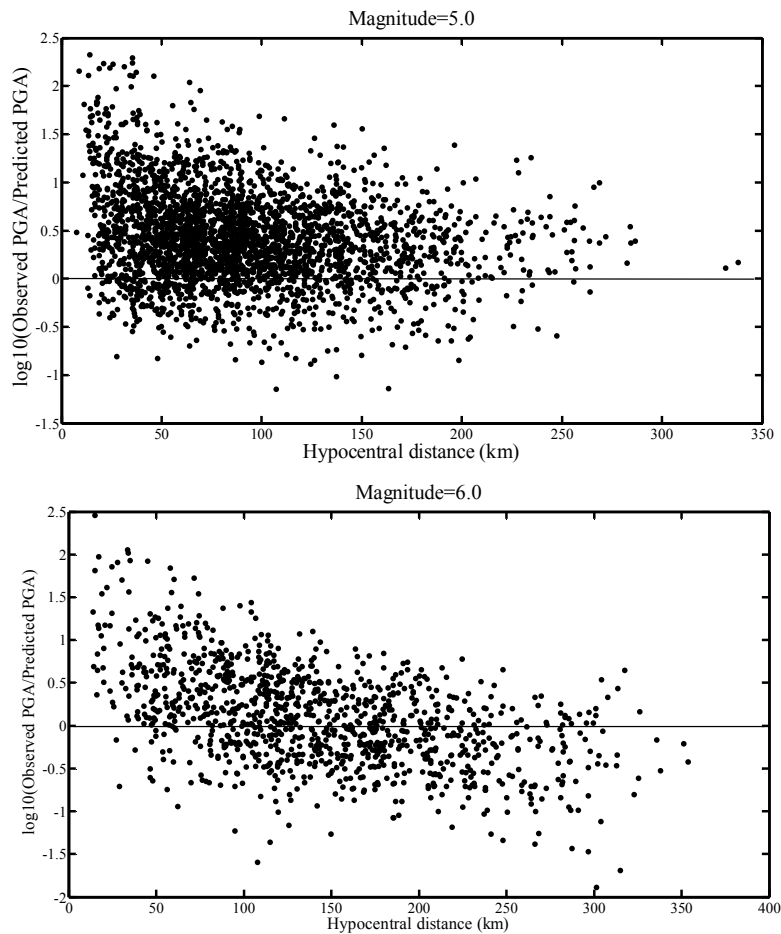
It is obvious that the mean residual of M_w 7.0 from this study is the lowest and that of M_w 6.0 is just higher than Fukushima's. The discreteness of these results, however, is the highest.

$$E = \frac{1}{N} \sum_{i=1}^N \log_{10} \left(\frac{\text{observed value}}{\text{predicted value}} \right) \quad (4.1)$$

$$\sigma = \sqrt{\frac{1}{N} \sum_{i=1}^N \left[\log_{10} \left(\frac{\text{observed value}}{\text{predicted value}} \right) \right]^2}$$

Table 4.1. Comparison of mean residuals and standard deviations

Relations	$M_w=5$		$M_w=6$		$M_w=7$	
	E	σ	E	σ	E	σ
Kanno (2006)	-0.0750	0.3710	-0.0717	0.3931	-0.0564	0.2956
Fukushima (1990)	-0.3257	0.4914	-0.1543	0.4192	0.0243	0.2874
Si, D=10km (2000)	0.0514	0.3667	0.0183	0.3855	-0.0300	0.2852
Si, D=20km (2000)	0.0124	0.3632	-0.0207	0.3856	-0.0690	0.2919
Si, D=30km (2000)	-0.0266	0.3640	-0.0597	0.3896	-0.1080	0.3035
This study	0.4292	0.6378	0.1062	0.5832	0.0585	0.4698



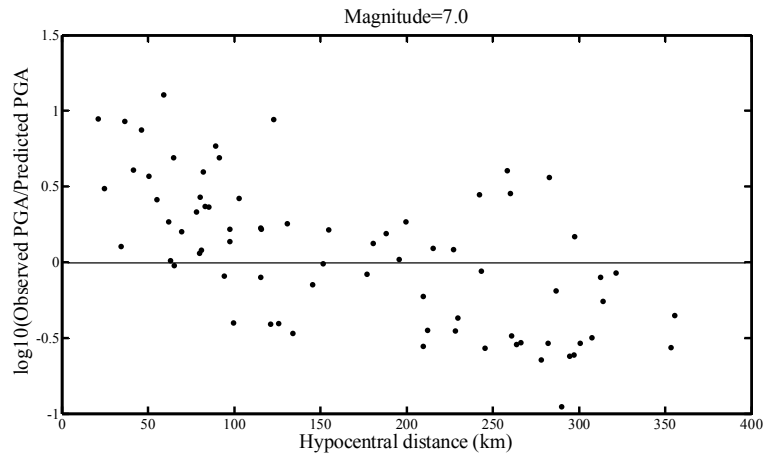


Figure 4.2. Mean residual with hypocentral distance

5. CONCLUSIONS

Regional source and crustal medium parameters of Tohoku area in Japan, the stress drop $\Delta\sigma$, the parameters indicating quality factor (Q_0 and η) and two piecewise-function points of the geometric spreading function R_1 and R_2 , are inverted by μ GA from small earthquakes ($M_w=3.5\sim 4.5$), recorded by a seismographic network F-net. The results are used to calculate Fourier spectra and simulate time histories. The median ground motions of 50-times simulations are adopted to construct the attenuation relationships. The results are compared with strong ground motion records of K-NET and several empirical relations. Generally speaking, the results are close to empirical relations, in some cases they are better than those, in other cases, they are worse.

ACKNOWLEDGEMENTS

This work was financially supported by National Nature Science Foundation of China (51178435 and 51178151) and International Science & Technology Cooperation Program of China (2011DFA21460).

REFERENCES

- Takamura, M. (1990). Magnitude-seismic moment relations for the shallow earthquakes in and around Japan. *Earthquake*. **43**: 257-265.
- Hanks, T.C. and Kanamori, H. (1979). A moment magnitude scale. *Journal of Geophysical Research*. **84**: 2348-2350.
- Boore, D.M. (2003). Simulation of ground motion using the stochastic method. *Pure and Applied Geophysics*. **160**: 635-676.
- Tao, Z., Tao X. and Wang X. (2012). Seismology based ground motion attenuation relationship for Sendai area. *Advanced Materials Research*. **382**: 7-11.
- Huo, J. and Hu Y. (1991). Study on envelop function of acceleration time history. *Earthquake Engineering and Engineering Vibration*. **11**: 1, 1-12.
- Fukushima, Y. and Tanaka, T. (1990). A new attenuation relation for peak horizontal acceleration of strong earthquake ground motion in Japan. *Bulletin of the Seismological Society of America*. **96**: 757-783.
- Kanno, T., Narita, A., Morikawa, N., Fujiwara, H. and Fukushima, Y. (2006). A new attenuation relation for strong ground motion in Japan based on recorded data. *Bulletin of the Seismological Society of America*. **96**: 879-897.
- Si, H. and Midorikawa, S. (2000). New attenuation relations for peak ground acceleration and velocity considering effects of fault type and site condition. *12th World Conference on Earthquake Engineering*. No.0532.
- Information on <http://www.fnet.bosai.go.jp/REGS/dataget/?LANG=en>, 2011.4
- Information on http://www.k-net.bosai.go.jp/k-net/search/index_en.html, 2011.4